Available online at www.sciencedirect.com
ScienceDirect
Chemical Physics Letters 449 (2007) 115–119
CHEMICAL PHYSICS LETTERS
www.elsevier.com/locate/cplett

The heterogeneous catalytic reaction $2A + B_2 \rightarrow 2AB$ exactly solved on a small lattice

P. Bergero, V. Pastor, I.M. Irurzun, E.E. Mola *

Instituto de Investigaciones Fisicoquímicas Teóricas y Aplicadas (INIFTA – CONICET), Facultad de Ciencias Exactas, Universidad Nacional de La Plata, Casilla Correo 314, La Plata 1900, Argentina

Received 10 August 2007; in final form 16 October 2007
Available online 22 October 2007

Abstract

We studied a kinetic model of a generic heterogeneous catalytic reaction $2A^* + B_2^* \rightarrow 2AB_g$. This reaction includes the steps of adsorption and desorption of reactants A and B_2, where B_2 requires two neighboring adsorption sites to be adsorbed. We solved the model exactly and without any restriction on a 2×2 lattice. Despite the reduced number of sites employed, the solution shows the main general features observed by simulating the mechanism on a large $N \times N$ lattice.

This result should encourage the search for an analytical solution as a reliable form to unravel details of a chemical reaction prior to performing numerical simulations.

1. Introduction

There are several examples of heterogeneous chemical reactions where chemical species require more than one adsorption site as a prerequisite to be adsorbed. This fact breaks down the equivalence between empty and occupied sites. Examples of this kind of reaction might be CO oxidation on Pt{1 0 0} [1,2], where the O_2 requires two neighboring sites to be adsorbed, whereas the CO molecule requires only one, and the $NO + H_2$ reaction on Rh{1 1 0} [3] and on Pt{1 1 0} [4]. In these reactions both oxygen and hydrogen desorptions also require two occupied neighboring sites.

These reactions show complex spatiotemporal behavior where the metal surface exhibits temporal and spatial oscillatory behavior, and much effort has been devoted to simulate them. The approaches are usually performed assuming the adsorbed overlayer to be infinite. However, practically important catalytic reactions often occur on very small (~10 nm) supported crystalline metal particles and there are simulations focused on interpreting the kinetic characteristics of chemical reactions confined in such a small space [2,5–8]. An important aspect is that the reactivity of small metal particles (typically, a few nm in size), which are present on supported catalysts, differs from those of macroscopic single-crystal planes. The small metal particles exhibit facets with different orientations. Due to the small dimensions of the facets, which typically comprise only a few hundred to a few thousand surface atoms, reaction-induced fluctuations will become important. For this reason it is important to study heterogeneous reactions on small lattices, in order to find the essential features of the mechanism that can even be found in such systems [3]. In all these studies the basic mechanism to understand the kinetic aspects of the reaction involves adsorption, desorption, diffusion and reaction steps, and the stoichiometric reaction can be represented as $2A + B_2 \rightarrow 2AB$.

In the present Letter, we exactly solve the heterogeneous catalytic reaction $2A + B_2 \rightarrow 2AB$ on a small lattice and show the calculation of averaged quantities such as the reaction rate and the fractional surface coverages. Results are compared with Monte Carlo simulations.

* Corresponding author. Fax: +54 221 425 46 42.
E-mail address: eemola@inifta.unlp.edu.ar (E.E. Mola).

0009-2614/$ - see front matter © 2007 Elsevier B.V. All rights reserved.
doi:10.1016/j.cplett.2007.10.049

The Letter is organized as follows: in Section 2, the model reaction is presented. This mechanism is not intended to represent that of any actual catalytic reaction, instead we selected the model to characterize a generic, bimolecular Langmuir–Hinshelwood reaction. Average reaction rate and fractional surface coverages are derived in Section 2. In Section 3, results and conclusions are presented.

2. The model

The heterogeneous reaction model proceeds through a Langmuir–Hinshelwood mechanism

$$A_{(g)} + * \rightarrow A^* \quad k_a,\ S \tag{1}$$

$$A^* \rightarrow A_{(g)} + * \quad k_d \tag{2}$$

$$B_{2(g)} + 2* \rightarrow 2B^* \quad k_a,\ S \tag{3}$$

$$B^* + B^* \rightarrow B_{2(g)} + 2* \quad k_d \tag{4}$$

$$A^* + B^* \rightarrow AB_{(g)} + 2* \quad k_r \tag{5}$$

where k_a, k_d and k_r are the rate constants for adsorption, desorption and reaction, respectively, $*$ denotes a vacant site on the catalyst surface and S stands for the sticking coefficient probability. This mechanism is not intended to represent that of any actual catalytic reaction but to select a model to characterize a generic bimolecular Langmuir–Hinshelwood reaction. The subindex (g) represents a molecule in the gaseous phase, and a superindex $*$ stands for adsorbed species. A molecules require single adsorption sites in order to be adsorbed (see Eq. (1)), whereas B_2 molecules require two neighboring lattice sites to be adsorbed (see Eq. (3)). The reaction step of Eq. (5) requires the existence of two neighboring sites occupied by different adsorbates to be accomplished. Desorption of B_2 molecules is a second order process and requires the existence of two neighboring lattice sites occupied by B^* adsorbates.

In the adsorption steps, Eqs. (1) and (3), we introduced a sticking coefficient S, which is the probability of a molecule to be adsorbed after the first impact on an adsorption site. If the sticking coefficient is less than one ($S < 1$), there will be the possibility of finding microstates with empty sites.

The desorption steps, Eqs. (2) and (4), and the reaction step, Eq. (5), are controlled by rate equations k_d and k_r.

If a lattice site is occupied, there is a probability P_d of desorption of that species if conditions given by Eqs. (2) and (4) are fulfilled, that is, if the lattice site is occupied by an adsorbate A, it is desorbed with probability P_d, but if the lattice site is occupied by an adsorbate B, the desorption will occur if a nearest neighbor site is also occupied by another B adsorbate (see Eq. (4)). In the first case, the vacant site is occupied with probability S by an adsorbate A, whereas in the second case both sites are occupied with probability $S/2$ either by two A or two B adsorbates to fulfil the requirements of Eq. (3). There will be a probability $1 - S$ that both sites will remain empty.

If a lattice site is an isolated vacancy, there is a probability (sticking coefficient) S of being occupied by an adsorbate A (or $1 - S$ of remaining empty). But if there is at least a nearest neighbor vacancy, then both sites are occupied with probability $S/2$ either by two A or two B adsorbates to meet the requirements of Eq. (3). There will be a probability $1 - S$ that both sites will remain empty.

The desorption probability P_d is one of the adjustable parameters in our model, and defines the relative rates of desorption to surface reaction

$$P_d = \frac{k_d}{k_r + k_d} \tag{6}$$

To compare our model with known experimental results we assume an Arrhenius dependence of the rate constants, $k_i = \nu_i \exp\left[-\frac{E_i}{kT}\right]$, where i stands for (d or r) desorption or reaction, respectively. In the $NO + H_2/Pt\{100\}$ and $CO + O_2/Pt\{100\}$ reactions [4,9–12], a typical value of the activation desorption energy is $E_d \approx 100$ kJ/mol, and the pre-exponential factor $\nu_d \approx 10^{-13}\ s^{-1}$. Reaction activation energies are lower than the desorption ones, and $E_r \approx 65$ kJ/mol might be a reasonable value together with $\nu_r \approx 10^{-9}\ s^{-1}$. The above-mentioned reactions were studied in a wide temperature range (300–600 K), and therefore, the values of our control parameter $P_d = k_d/(k_r + k_d)$ at the temperature values $T = 350$, 400, 450, 500 and 550 K, are $P_d = 0.056$, 0.211, 0.463, 0.687 and 0.825, respectively.

The second adjustable parameter in our model is the sticking coefficient S, which stands for the adsorption probability, after the first impact, of a gaseous molecule on the substrate surface.

For both CO and O_2 on $Pt\{100\}$, values of $S = 0.89$ and 0.28, respectively, have been reported at low coverages [10]. A dependence of S on the number and chemical nature of neighboring particles (i.e., of the microstate) was not considered in the present work for simplicity. This is equivalent to assuming a constant sticking probability rather than a coverage dependent one. Also in order to simplify the mathematical analysis (see below the probability matrix construction) in the present work we assumed equal values of S for both A and B species.

To represent the catalytic surface, we used a square 2×2 lattice, and periodic boundary conditions were imposed. Fig. 1 shows the 21 (twenty-one) different microstates that can be observed with degeneracies $g_1 = 2$, $g_2 = 4$, $g_3 = 4$, $g_4 = 4$, $g_5 = 1$, $g_6 = 1$, $g_7 = 4$, $g_8 = 8$, $g_9 = 4$, $g_{10} = 4$, $g_{11} = 8$, $g_{12} = 4$, $g_{13} = 4$, $g_{14} = 8$, $g_{15} = 4$, $g_{16} = 2$, $g_{17} = 4$, $g_{18} = 2$, $g_{19} = 4$, $g_{20} = 4$ and $g_{21} = 1$. By choosing equal values of partial pressure for reactants A and B_2 (i.e., $p_A = p_{B_2} = 0.5$), the probability p_i of a macroscopic state was given by $p_i = g_i/81$. The origin of normalization factor *81* is due to the fact that we have three different options to place in each lattice site, and therefore $81 = 3^4$.

As time elapses, the surface state changes and therefore there is a probability P_{ij} for the transition from states i to j. All these transition probabilities can be collected in a 21×21 matrix called the transition probability matrix. As an example, in Fig. 2 we show all the transition probabilities starting from microstate 11. The four main branches in

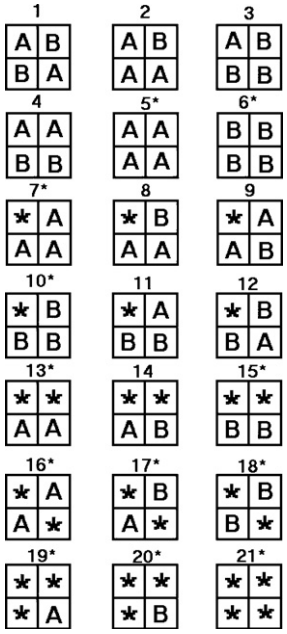

Fig. 1. The 21 different microstates that can be observed in our model on a 2×2 square lattice with periodic boundary conditions.

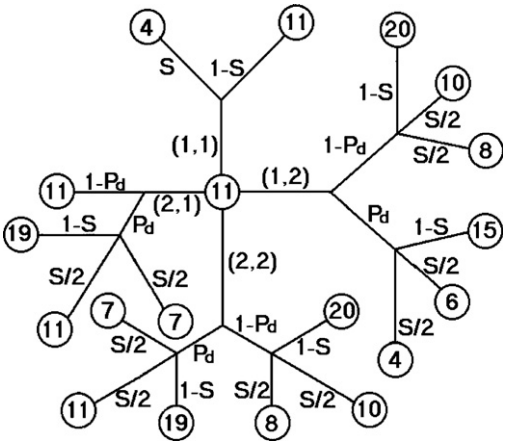

Fig. 2. The transition probabilities starting from microstate 11 (see Fig. 1).

this figure correspond to every lattice site visited in a clockwise sense. From that figure we obtain the matrix elements of the 11th row of the matrix P_{ij}. The non-zero matrix elements are: $P_{11,4}=\frac{1}{4}S\left(1+\frac{1}{2}P_{\mathrm{d}}\right)$, $P_{11,6}=\frac{1}{8}SP_{\mathrm{d}}$, $P_{11,7}=\frac{1}{4}SP_{\mathrm{d}}$, $P_{11,8}=\frac{1}{4}S(1-P_{\mathrm{d}})$, $P_{11,10}=\frac{1}{4}S(1-P_{\mathrm{d}})$, $P_{11,11}=\frac{1}{4}(2+SP_{\mathrm{d}}-S-P_{\mathrm{d}})$, $P_{11,15}=\frac{1}{4}P_{\mathrm{d}}(1-S)$, $P_{11,19}=\frac{1}{2}P_{\mathrm{d}}(1-S)$, $P_{11,20}=\frac{1}{2}(1-P_{\mathrm{d}})(1-S)$.

In an analogous way, the non-zero matrix elements of the remaining 20 rows of the probability matrix can be derived. From the transition probability matrix, averaged quantities such as the average reaction rate and the average surface coverages can be calculated.

Let e_{ik} be the probability of arriving at microstate i in k steps. If $k=0$,

$$e_{i0}=p_i,\quad i=1,2,\ldots,21 \tag{7}$$

If $k>0$,

$$e_{ik}=\sum_{j=1}^{21}e_{jk-1}P_{ji},\quad i=1,2,3,\ldots21 \tag{8}$$

where both indexes i and j run over the whole set of microstates (1, 2, 3, ... 21). P_{ji} stands for the probability of arriving at microstate i from microstate j in one step.

Let $X(k)$ be a random variable, which is defined as follows, $X(k)=1$ if there is reaction at step k, and $X(k)=0$ otherwise. The average reaction rate $\langle v\rangle$ over n steps can be defined as follows:

$$\langle v\rangle=\frac{1}{n}Z(n) \tag{9}$$

where

$$Z(n)=\sum_{k=0}^{n}X(k) \tag{10}$$

with $Z(n)$ being the number of molecules produced over n steps. If v_i ($i=1,\ 2,\ldots21$) is the probability of reaction at the ith microstate, we have: $v_1=1-P_{\mathrm{d}}$, $v_2=\frac{3}{4}(1-P_{\mathrm{d}})$, $v_3=\frac{3}{4}(1-P_{\mathrm{d}})$, $v_4=1-P_{\mathrm{d}}$, $v_8=\frac{1}{2}(1-P_{\mathrm{d}})$, $v_9=\frac{3}{4}(1-P_{\mathrm{d}})$, $v_{11}=\frac{1}{2}(1-P_{\mathrm{d}})$, $v_{12}=\frac{3}{4}(1-P_{\mathrm{d}})$, $v_{14}=\frac{1}{2}(1-P_{\mathrm{d}})$, and $v_i=0$ otherwise.

The average reaction rate at the kth step, $\langle v(k)\rangle$, is

$$\langle v(k)\rangle=E(X(k))=\sum_{i=1}^{21}e_{ik}v_i \tag{11}$$

Also let θ^{A}_{sk} (θ^{B}_{sk} or θ^{E}_{sk}) be the probability of finding s lattice sites occupied by adsorbates of type A (B or empty E) at the kth step, then

$$\theta^{\mathrm{A}}_{0k}=e_{6k}+e_{10k}+e_{15k}+e_{18k}+e_{20k}+e_{21k} \tag{12}$$
$$\theta^{\mathrm{A}}_{1k}=e_{3k}+e_{11k}+e_{12k}+e_{14k}+e_{17k}+e_{19k} \tag{13}$$
$$\theta^{\mathrm{A}}_{2k}=e_{1k}+e_{4k}+e_{8k}+e_{9k}+e_{13k}+e_{16k} \tag{14}$$
$$\theta^{\mathrm{A}}_{3k}=e_{2k}+e_{7k} \tag{15}$$
$$\theta^{\mathrm{A}}_{4k}=e_{5k} \tag{16}$$

Analogously,

$$\theta^{\mathrm{B}}_{0k}=e_{5k}+e_{7k}+e_{13k}+e_{16k}+e_{19k}+e_{21k} \tag{17}$$
$$\theta^{\mathrm{B}}_{1k}=e_{2k}+e_{8k}+e_{9k}+e_{14k}+e_{17k}+e_{20k} \tag{18}$$
$$\theta^{\mathrm{B}}_{2k}=e_{1k}+e_{4k}+e_{11k}+e_{12k}+e_{15k}+e_{18k} \tag{19}$$
$$\theta^{\mathrm{B}}_{3k}=e_{3k}+e_{10k} \tag{20}$$
$$\theta^{\mathrm{B}}_{4k}=e_{6k} \tag{21}$$

and

$$\theta^{\mathrm{E}}_{0k}=e_{1k}+e_{2k}+e_{3k}+e_{4k}+e_{5k}+e_{6k} \tag{22}$$
$$\theta^{\mathrm{E}}_{1k}=e_{7k}+e_{8k}+e_{9k}+e_{10k}+e_{11k}+e_{12k} \tag{23}$$
$$\theta^{\mathrm{E}}_{2k}=e_{13k}+e_{14k}+e_{15k}+e_{16k}+e_{17k}+e_{18k} \tag{24}$$
$$\theta^{\mathrm{E}}_{3k}=e_{19k}+e_{20k} \tag{25}$$
$$\theta^{\mathrm{E}}_{4k}=e_{21k} \tag{26}$$

Let θ_s^A $(s = 0, 1, \ldots, 4)$ be the probability of finding s lattice sites occupied by adsorbates of type A when the number of steps tends to infinity

$$\theta_s^A = \mathrm{Lim}_{k\to\infty}\theta_{sk}^A \tag{27}$$

The average fractional surface coverage $\langle\theta^A\rangle$ can be evaluated as follows:

$$\langle\theta^A\rangle = \frac{1}{4}\sum_{s=0}^{4} s\theta_s^A \tag{28}$$

and its standard deviation can be defined as follows:

$$\sigma(\langle\theta^A\rangle) = \left[\sum_{s=0}^{4}\theta_s^A\left(\frac{s}{4} - \langle\theta^A\rangle\right)^2\right]^{1/2} \tag{29}$$

In an analogous way, $\langle\theta^B\rangle$, $\langle\theta^E\rangle$, $\sigma(\langle\theta^B\rangle)$ and $\sigma(\langle\theta^E\rangle)$ can be defined.

3. Results and conclusions

The numerical predictions of the model were studied in the present work and compared with those obtained by Monte Carlo simulations. The set of 21 microstates shown in Fig. 1 can be divided into two sets: Set A is formed by microstates 1, 12 and 18, and Set B is formed by the remaining microstates. Starting from any element of Set A, the 21 microstates (i.e., A ∪ B) can be generated in a few steps, while starting from any element of Set B, only the elements of Set B are generated. The reason for this division lies in the transition matrix probability; if the control parameters S and P_d are different from 0 or 1, we have

$$P_{ij} \neq 0, \quad i \in A, \quad j \in B \tag{30}$$

and

$$P_{ji} = 0, \quad i \in A, \quad j \in B \tag{31}$$

Therefore

$$\mathrm{Lim}_{k\to\infty}e_{ik} = e_{i\infty} = 0, \quad i \in A \tag{32}$$

and

$$\mathrm{Lim}_{k\to\infty}e_{jk} = e_{j\infty} \neq 0, \quad j \in B \tag{33}$$

After overcoming a transient and independently of the starting distribution of microstates, we arrive to a *unique final distribution of microstates probabilities*, dependent only on the control parameters (S and P_d) values employed in the transition matrix probability and given by

$$e_{j\infty} = f(S,\ P_d), \quad j \in B \tag{34}$$

$$e_{i\infty} = 0, \quad i \in A \tag{35}$$

As a result of the above-derived conclusions, *both the average reaction rate* $\langle v\rangle$ *and the average coverage* $\langle\theta^A\rangle$ (or $\langle\theta^B\rangle$ or $\langle\theta^E\rangle$) *when the number of steps* $k \to \infty$ *are independent of the initial distribution of microstates probabilities*. From the experimental point of view, this means that $\langle v\rangle$ and $\langle\theta^A\rangle$ (or $\langle\theta^B\rangle$ or $\langle\theta^E\rangle$) are independent of the initial surface coverage and even of the initial distribution of adsorbates.

Fig. 3a shows the dependence of the average reaction rate $\langle v\rangle$ on the desorption probability P_d at a constant value of the sticking coefficient probability S. A maximum $\langle v\rangle_{max}$ is seen when the desorption rate P_d competes with surface reaction $1 - P_d$, i.e., by assuming equal values of partial pressures of the reactants, there exists a temperature value that ensures a maximum average reaction rate.

Fig. 3b shows the dependence of $\langle v\rangle$ on S at a constant P_d value. A maximum $\langle v\rangle_{max}$ is also seen in this figure because there is an optimum reactive microstate probability distribution. From Fig. 1, we see that there are nine reactive microstates, two (1) and (12) out of the three microstates of Set A, and seven (2)–(4), (8), (9), (11) and (14) out of the 18 microstates of Set B. When the number of steps $k \to \infty$, the number of reactive microstates is reduced to seven, all of them belonging to Set B and contributing to the average reaction rate. If the sticking probability S is increased

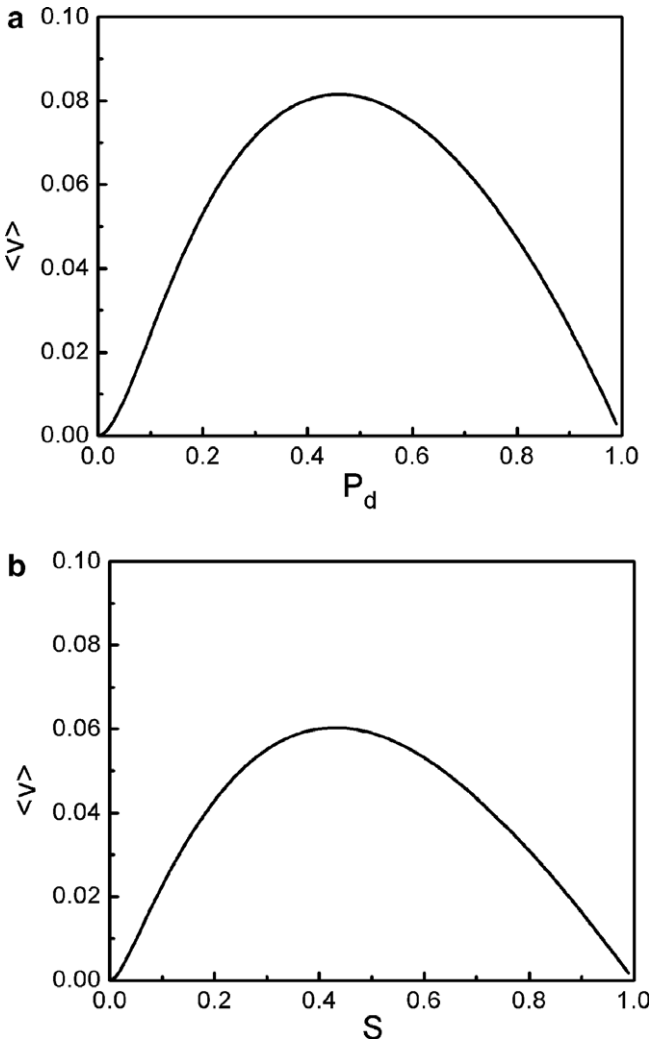

Fig. 3. (a) Dependence of the average reaction rate $\langle v\rangle$ on the desorption probability P_d at a constant value of the sticking coefficient probability $S = 0.6$. (b) Dependence of $\langle v\rangle$ on S at a constant value of $P_d = 0.2$.

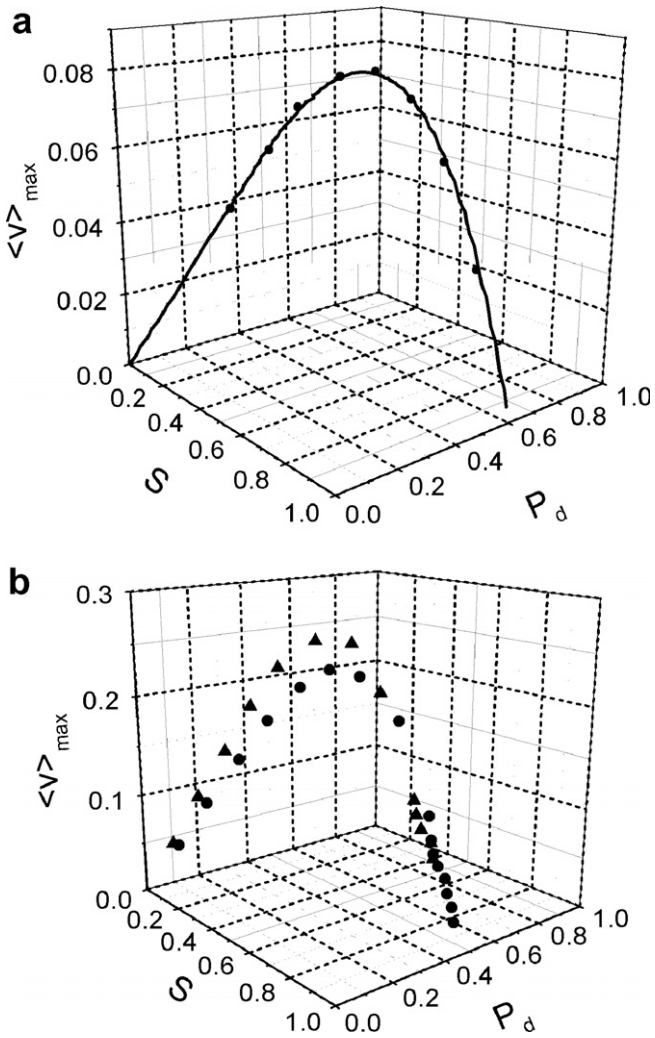

Fig. 4. (a) Three-dimensional plot of $\langle v\rangle_{max}$ vs both S and P_d in a 2×2 square lattice (line). $\langle v\rangle_{max}$ has an absolute maximum at $S=0.58$ and $P_d=0.45$. Symbols indicate the results obtained by a Monte Carlo simulation employing 5×10^7 Monte Carlo steps. (b) Monte Carlo simulations performed on 4×4 (circles) and 8×8 (triangles) square lattices.

($S\to1$), the most contributing reactive microstates are three (2)–(4) and $\langle\theta^A\rangle+\langle\theta^B\rangle\to1$. Alternatively, when S is reduced ($S\to0$), the probability of those microstates with 2, 3 or 4 empty sites will be increased and between them there is only one reactive microstate (14). Therefore, there will be an intermediate S value where an optimum reactive distribution of microstate probabilities is achieved to obtain a maximum average reaction rate $\langle v\rangle_{max}$.

Fig. 4a shows a three-dimensional plot of $\langle v\rangle_{max}$ versus both S and P_d. From that figure we see that $\langle v\rangle_{max}$ has an absolute maximum at $S=0.58$ and $P_d=0.45$. For comparison purposes, in the same figure we show the remarkable agreement with a Monte Carlo simulation employing 5×10^7 Monte Carlo steps.

Monte Carlo simulations can be used to study the reaction characteristics on larger lattices. Fig. 4 shows simulations performed on 4×4 and 8×8 lattices. In both examples a similar pattern, such as the one obtained solving exactly a 2×2 lattice, is observed.

Despite the reduced number of sites employed, the solution shows the main general features observed by simulating the mechanism on a large $N\times N$ lattice. This result should encourage the search for an analytical solution as a reliable form to unravel details of a chemical reaction prior to performing numerical simulations.

Acknowledgements

This work was financially supported by the Consejo Nacional de Investigaciones Científicas y Técnicas CONICET, Universidad Nacional de La Plata, UNLP, and Agencia Nacional de Promoción Científica y Tecnológica, ANPCyT.

References

[1] M. Gruyters, D.A. King, J. Chem. Soc., Faraday Trans. 93 (1997) 2947.
[2] Yu. Suchorski, J. Beben, R. Imbihl, E.W. James, Da-Jiang Liu, J.W. Evans, Phys. Rev. B 63 (2001) 165417.
[3] A. Makeev, M. Hinz, R. Imbihl, J. Chem. Phys. 114 (2001) 9083.
[4] S.J. Lombardo, T. Fink, R. Imbihl, J. Chem. Phys. 98 (1993) 5526.
[5] V.P. Zhdanov, B. Kasemo, Phys. Rev. B 62 (2000) R4849.
[6] V.P. Zhdanov, B. Kasemo, Phys. Rev. E 61 (2000) R2184.
[7] F. Chavez, L. Vicente, A. Perera, M. Moreau, J. Chem. Phys. 112 (2000) 8672.
[8] J. Cortes, E. Valencia, P. Araya, J. Chem. Phys. 109 (1998) 5607.
[9] M. Gruyters, A.T. Pasteur, D.A. King, J. Chem. Soc., Faraday Trans. 92 (1996) 2941.
[10] M. Gruyters, T. Ali, D.A. King, J. Phys. Chem. 100 (1996) 14417.
[11] H. Uecker, R. Imbihl, M. Rafti, I.M. Irurzun, J.L. Vicente, E.E. Mola, Chem. Phys. Lett. 382 (2003) 232.
[12] I.M. Irurzun, E.E. Mola, R. Imbihl, Chem. Phys. 323 (2006) 295.